

Broadband multimode antenna and its array for wireless communication base stations

Rui Wu  | Qing-Xin Chu 

School of Electronic and Information Engineering, South China University of Technology, Guangzhou, China.

Correspondence

Rui Wu, School of Electronic and Information Engineering, South China University of Technology, Guangzhou, China.

Email: wurui@scut.edu.cn

Funding Information

This work was supported in part by the National Nature Science Foundations of China (61671207), Project funded by China Postdoctoral Science Foundation (2018M643084) the Guangdong Technology Equipment Project ([2015] 1303), and the Guangzhou Science Technology Project (201604016087).

A wideband dual-polarized antenna coupling cross resonator is proposed for LTE700/GSM850/GSM900 base stations. An additional resonance is introduced to obtain strong coupling between the dipole and resonator. Moreover, the input impedance of the proposed antenna is steadily close to $50\ \Omega$, which results in better impedance matching. Therefore, a wide bandwidth can be achieved with multi-resonance. A prototype is fabricated to verify the proposed design. The measured results show that the antenna has a fractional bandwidth of 35.7% from 690 MHz to 990 MHz for $|S_{11}| < -15\ \text{dB}$. Stable radiation patterns as well as gain are also obtained over the entire operating band. Moreover, a five-element antenna array with an electrical downtilt of 0° to 14° is developed for modern base station applications. Measurement shows that a wide impedance bandwidth of 34.7% (690 MHz to 980 MHz), stable HPBW (3-dB beamwidth) of $65 \pm 5^\circ$, and high gain of $13.8 \pm 0.6\ \text{dBi}$ are achieved with electrical downtilts of 0° , 7° , and 14° .

KEYWORDS

Antenna Array, Broadband, Dual-Polarized, Electrical Downtilt, Multimode, Resonator

1 | INTRODUCTION

With the significant development of wireless communication systems, dual-polarized antennas are widely used in base stations to reduce the effects of multipath fading and increase signal reliability [1–4]. Dual-polarized antennas have aroused considerable attention in recent years [5–11]. With the rapid development of long-term evolution (LTE), the 700 MHz band has become one of the international mainstreams for LTE. Compared to other bands, the LTE700 band has advantages such as relatively longer wavelength, larger signal coverage, powerful penetration, and low cost of networking, which are of great significance. Therefore, the lower frequency bandwidth for base stations has been further extended to 698 MHz to 960 MHz in combination with the high-quality frequency band LTE700. Consequently, broadband dual-polarized antennas for 698 MHz to 960 MHz have become

desirable. Recently, an increasing number of antennas have been proposed for GSM850/GSM900 base stations [12–19]. However, they are still not wide enough to cover LTE700/GSM850/GSM900 with dual-polarization. Several techniques have been proposed for impedance bandwidth enhancement such as meandering probe feed [20] and multiparasitic resonator [21]. Moreover, broadband multidipole antennas have been proposed for obtaining a stable beam width [22]. However, they have the disadvantage of being bulky. In addition, antenna arrays are needed for real base station applications [23,24]. Therefore, it is challenging as well as of great significance to design a wideband dual-polarized antenna array with stable radiation patterns for base station applications.

In this paper, a broadband dual-polarized antenna for LTE700/GSM850/GSM900 base station is presented. By employing a cross resonator, a new resonance is introduced. The real part of the input impedance (input resistance) at

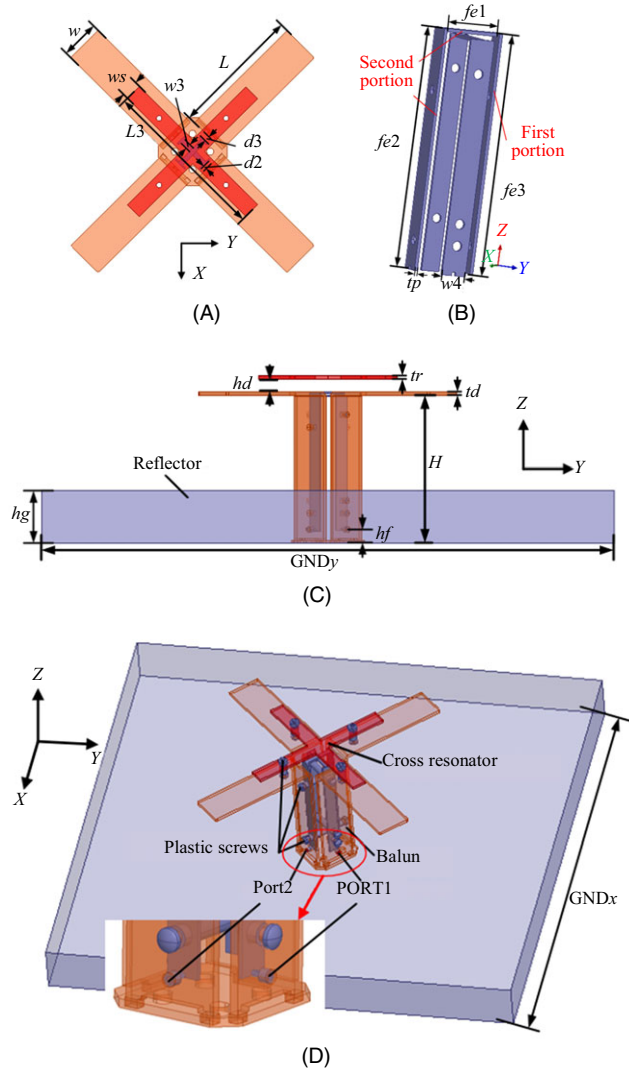


FIGURE 1 Antenna configurations (A) top view, (B) feeding structures, (C) side view, (D) 3D view

TABLE 1 Optimized design parameters of the proposed antenna

Parameter	GNDx	GNDy	H	L
Value (mm)	345	345	85	77.6
Parameter	d3	ws	L3	fe1
Value (mm)	3.5	10	98	18.8
Parameter	fe2	fe3	d	hd
Value (mm)	77	78	26	7
Parameter	td	tp	w1	w2
Value (mm)	2	1	8	6
Parameter	w3	d2	d3	hf
Value (mm)	3	2.5	3.5	8

high frequencies can be steadily increased to about 50 Ω , and the imaginary part is steadily close to zero. Simultaneously, the zero point of the input impedance can be lowered

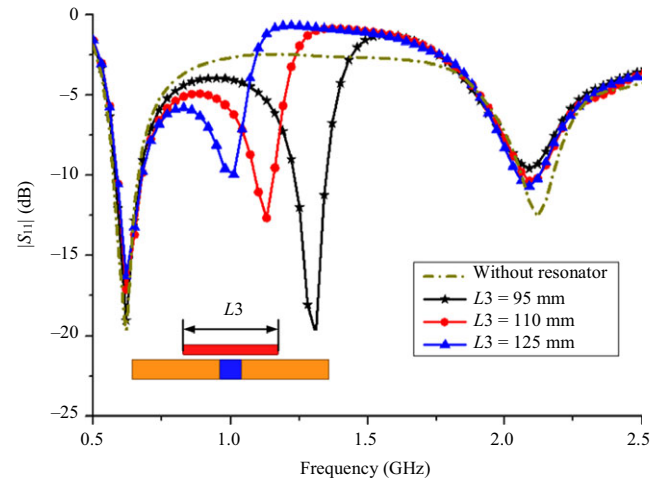


FIGURE 2 $|S_{11}|$ for resonator coupling dipole antenna with various L_3

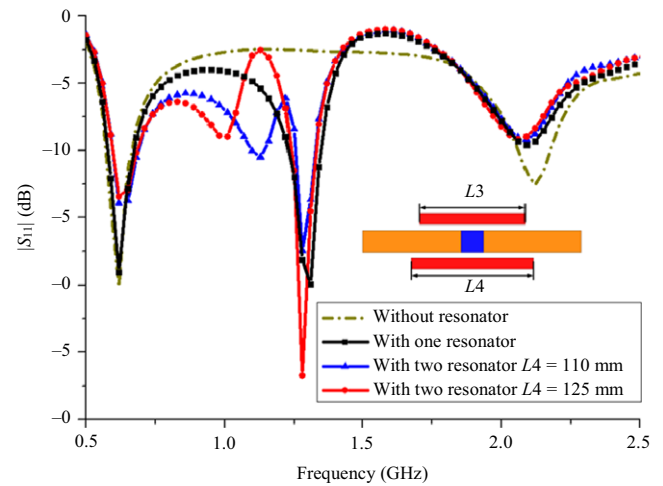


FIGURE 3 Comparison of resonator coupling dipole antenna

by properly adjusting the size and the position of the cross resonator. As a result, the new resonant point can be lowered toward the operating band. Moreover, the impedance matching between the two resonances is significantly improved at the same time. Thus, a wide impedance bandwidth can be achieved for wideband impedance matching and multiresonances within the desired operating band. Moreover, a five-element antenna array with various down-tilts is developed for real base station applications. Stable HPBW and gain are obtained over the desired operating band with electrical down tilts of 0°, 7°, and 14°.

2 | ANTENNA DESIGN

The configuration of a wideband dual-polarized antenna is illustrated in Figure 1. The proposed antenna consists of a

pair of $\pm 45^\circ$ orthogonally placed dipoles, a pair of U-shaped strip feed lines, baluns, a cross resonator, and a reflector. The baluns are connected with the dipole and the box-shaped reflector, and function as a balanced to unbalanced transformer. The cross resonator is placed over the dipole and is fixed by four plastic pillars with a height of hd . The length of the dipole $2L$ is first designed as 0.5λ , and the antenna is placed at a height of 0.25λ (λ is the wavelength at the center frequency of 820 MHz) upon the box-shaped reflector to obtain a unidirectional radiation pattern. The inner conductor of the coaxial cables (with a characteristic impedance of $50\ \Omega$) is connected with the end of the U-shaped feeding lines, whereas the outer conductors are soldered on the end of the balun at a short height of hf from the reflector. The U-shaped feeding lines consist of two portions, and are made by folding a metallic strip into a U-shape with a thickness of 1 mm. The first portion, which is a vertically placed transmission line, is connected with the inner conductor of the coaxial cable, and the other end of this portion is connected with the edge

of the second portion. The second portion is an L-shaped coupling strip line, which can be adjusted for the antenna impedance matching [25,26]. The antenna was simulated and optimized using ANSOFT HFSS [27]; the detailed parameters are listed in Table 1. The proposed wideband dual-polarized antenna was fabricated by metal casting, and it was then assembled and fixed together by plastic screws. The reflector was made of an aluminum alloy plate with a thickness of 2 mm and four holes at the center. Four metallic screws were used to fix the antenna through these four holes.

As shown clearly in Figure 2, a new resonant point is induced by the coupling resonator near the dipole. In addition, two new resonances are induced by the coupling resonators with two different sizes, as illustrated in Figure 3. Using a resonator-coupled dipole for multiresonance, a wide bandwidth can be achieved. Based on this theory, a multiresonance wideband dual-polarized antenna with a cross resonator is proposed. The input impedance and $|S_{11}|$ of the

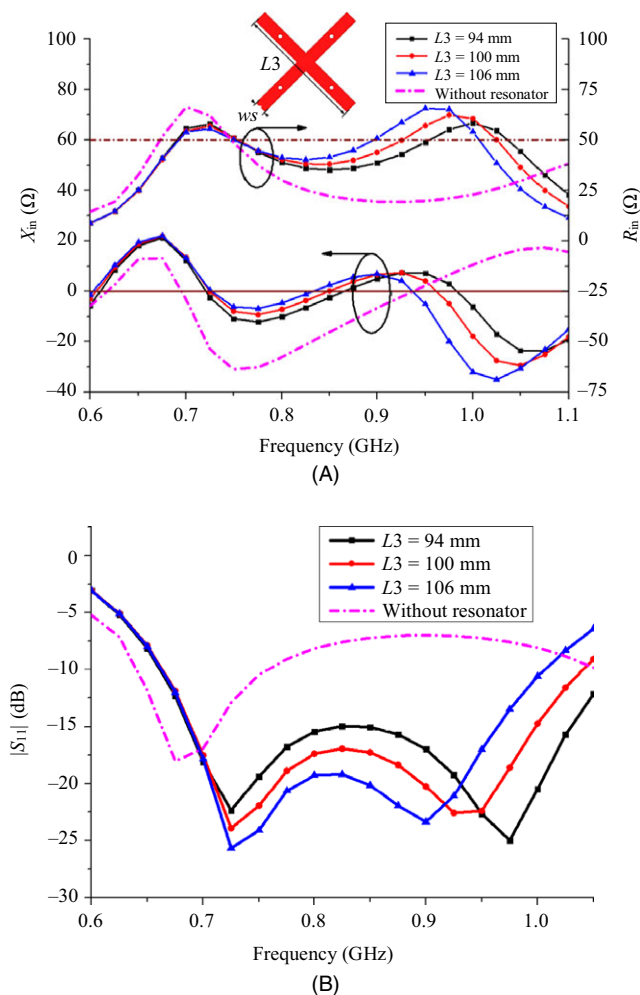


FIGURE 4 Input impedance and $|S_{11}|$ of the proposed antenna with different $L3$

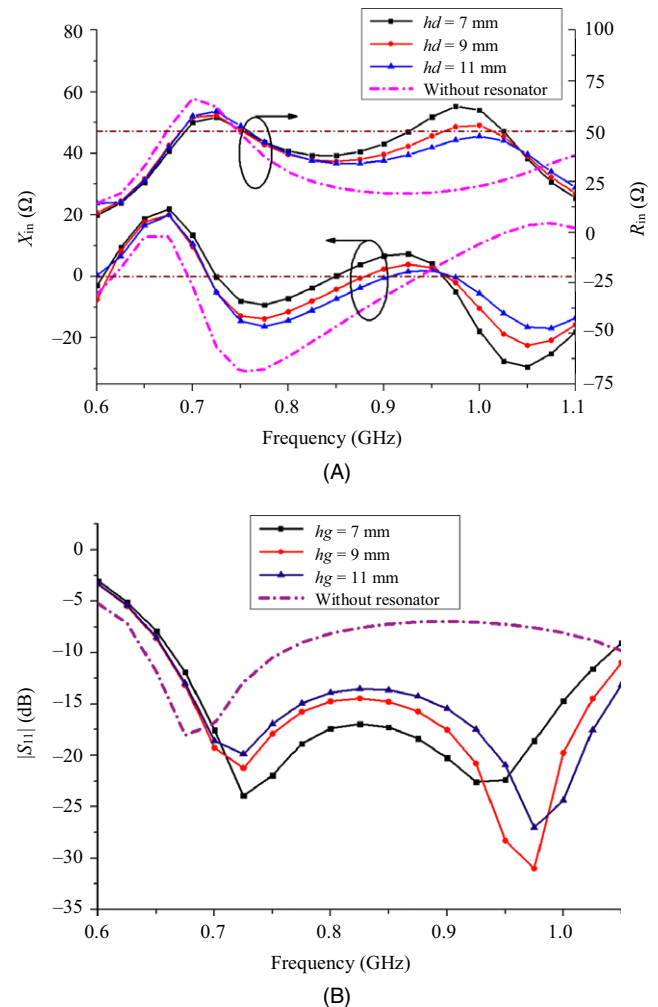


FIGURE 5 Input impedance and $|S_{11}|$ of the proposed antenna with different hd

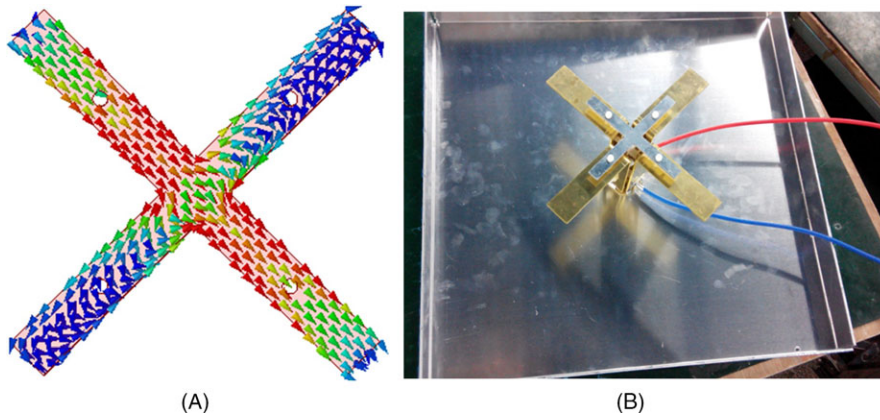


FIGURE 6 (A) Current distribution on the resonator when port 1 is excited, (B) photo of the proposed antenna

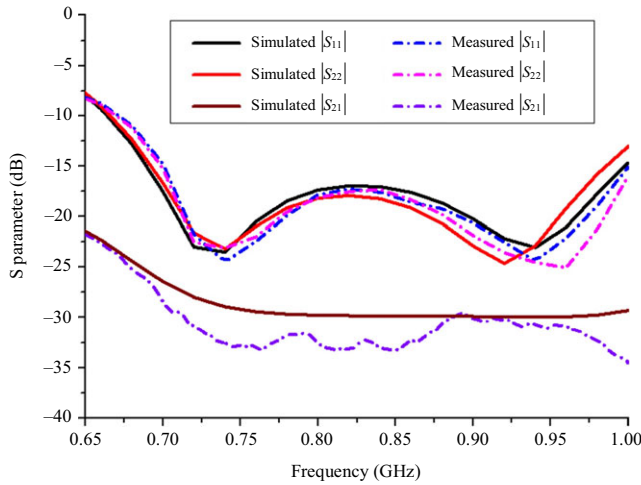


FIGURE 7 Simulated and measured $|S_{11}|$ and $|S_{21}|$ of the proposed antenna

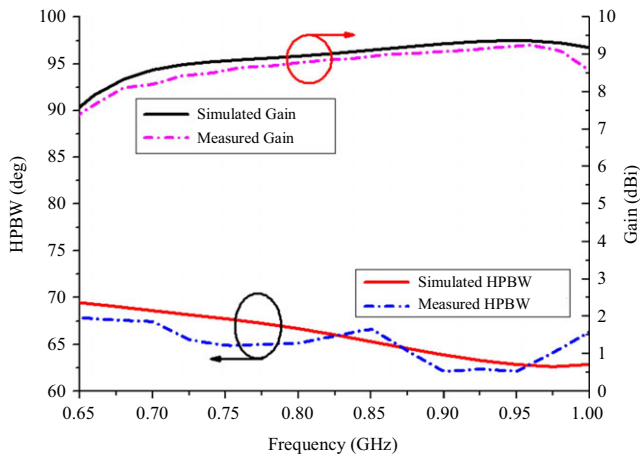


FIGURE 8 Simulated and measured Gain and HPBW (H -plane) of the antenna

proposed antenna with different sizes and positions of the cross resonator are illustrated in Figures 4 and 5, respectively. As shown in Figure 4, with an increase in L_3 (the length of the resonator), the input resistance is increased and becomes steadily close to 50Ω , especially around the

higher frequency of 950 MHz. On the other hand, the imaginary part of the input impedance is flatter and remains steadily close to zero, whereas the zero point of the input impedance moves toward the lower band. Therefore, there exist two resonant modes in the entire operating band, and impedance matching between the two modes is improved. As a result, a wide impedance bandwidth is achieved. Similarly, Figure 5 illustrates the input impedance and $|S_{11}|$ with various values of hd (the vertical distance of the resonator from the dipole). With a decrease in hd , the input impedance becomes steadily close to 50Ω , and the zero point of the imaginary part moves toward 950 MHz. Thus, a better impedance matching is obtained, and two resonant points are formed in the desired operating band, resulting in an enhanced impedance bandwidth. The current distribution on the cross resonator is shown in Figure 4A. It is clearly seen that when port 1 is excited, the current on the symmetric plane is almost null. Based on the above analysis and statements, the mechanisms of the proposed antenna can be explained as follows. In general, the lower resonant point is decided by the size of the dipole. Our desired operating band is 698 MHz to 960 MHz, and the input impedance is relatively far from 50Ω . Therefore, a narrow bandwidth and bad impedance matching are exhibited in the absence of a resonator. By employing a cross resonator, a new resonant mode is introduced and the impedance matching is improved over the operating band. We can move this mode by changing the size and position of the resonator. Since the lower resonant point is mainly decided by the size of the dipole, we can control the two resonant points almost independently. Therefore, multiresonance and good impedance matching in the desirable operating band can be achieved to form a wider impedance bandwidth.

3 | ANTENNA PERFORMANCE

A prototype was fabricated to verify the antenna element, as shown in Figure 6B. The measured results of the S parameters, antenna gain, and radiation patterns were

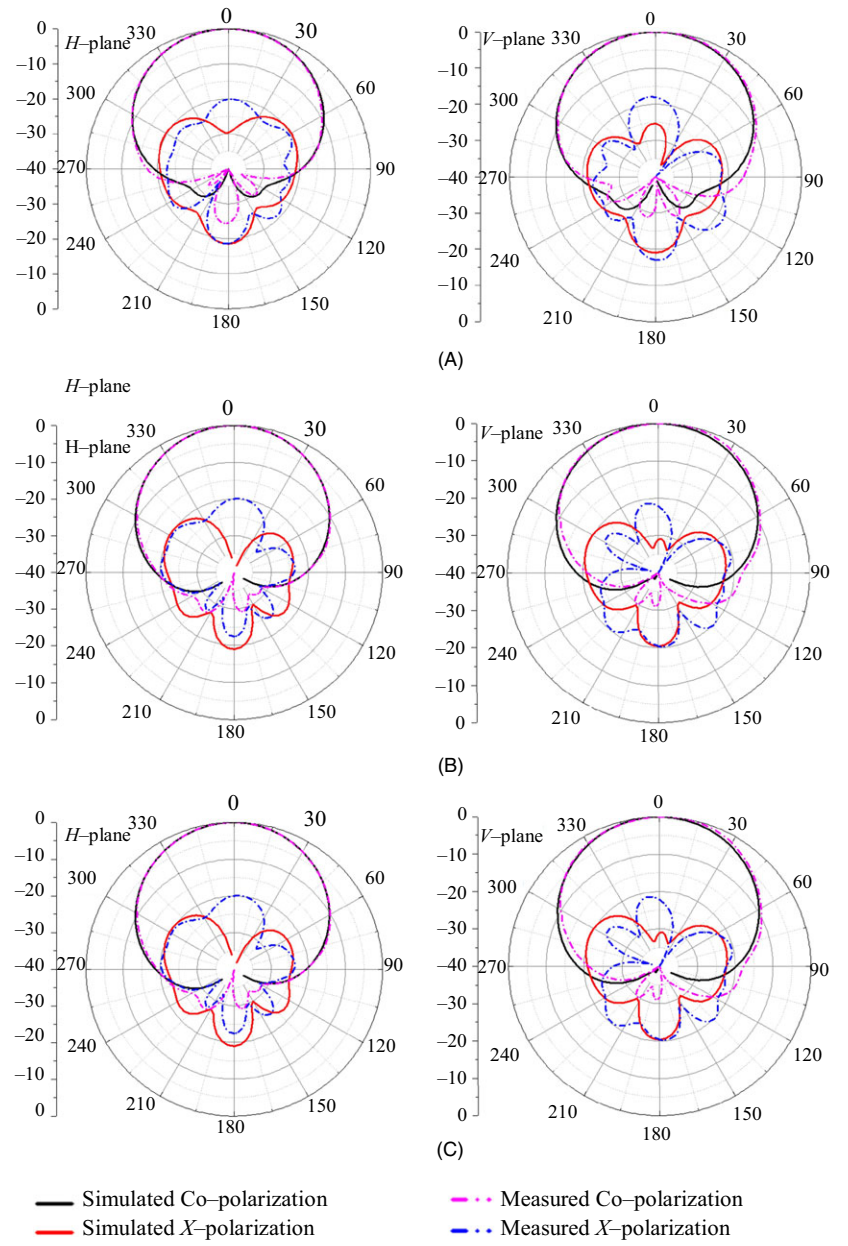


FIGURE 9 Simulated and measured radiation pattern for port 1 at (A) 700 MHz, (B) 850 MHz, and (C) 950 MHz, when port 1 is driven

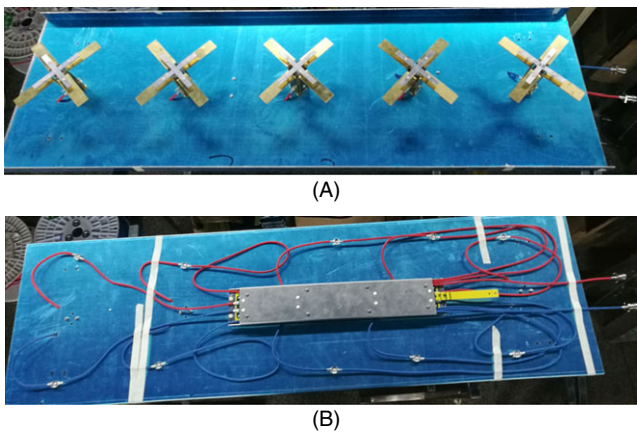


FIGURE 10 Prototype of the five-element antenna array

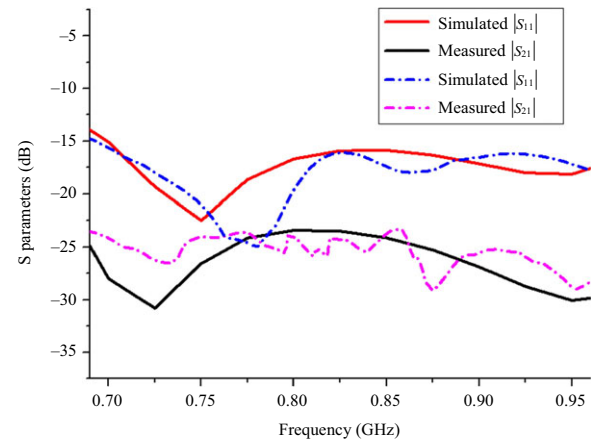


FIGURE 11 Simulated and measured S parameters of the antenna array with no downtilt

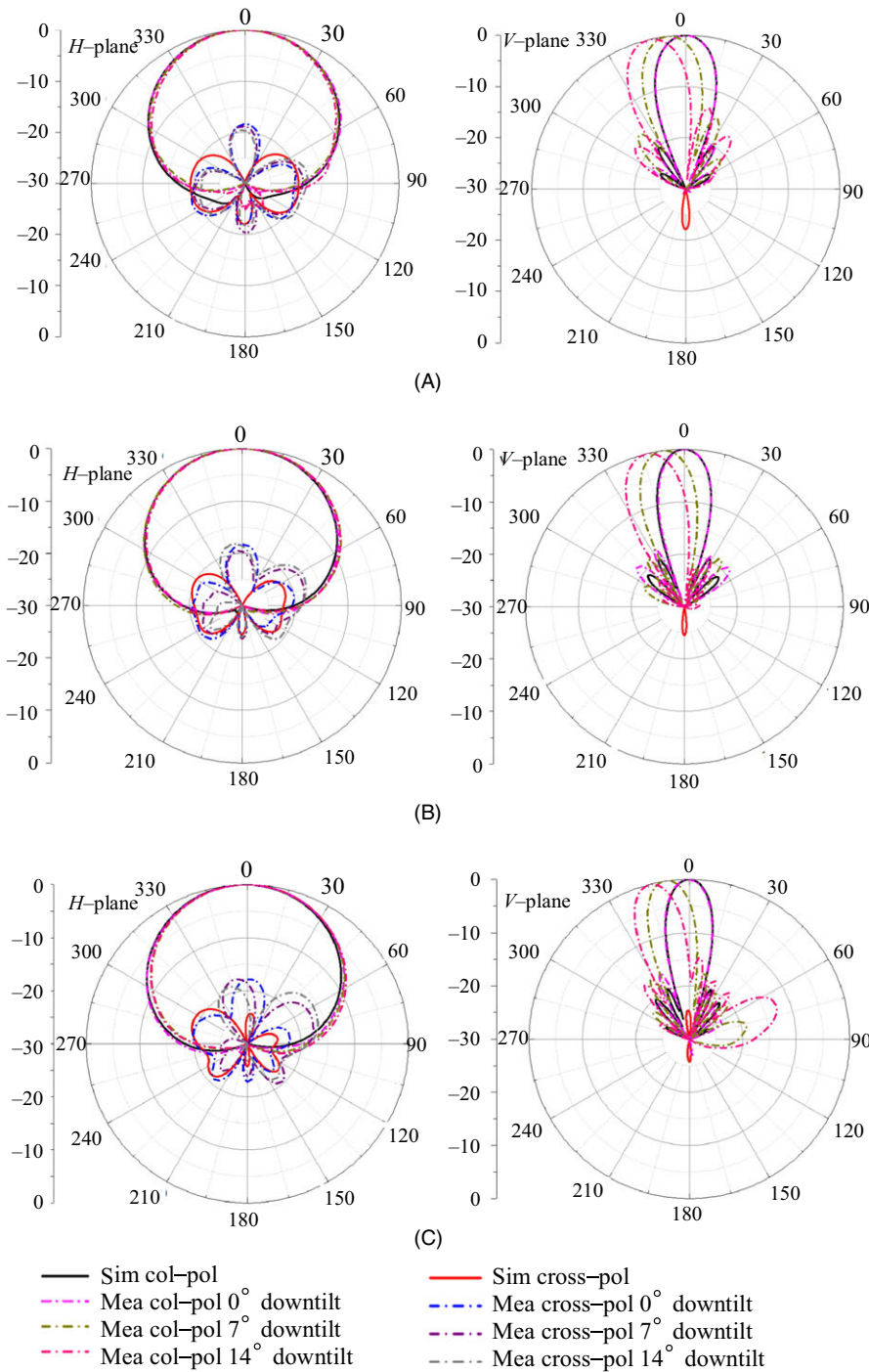


FIGURE 12 Simulated and measured radiation pattern of the antenna element at (A) 700 MHz, (B) 850 MHz, and (C) 950 MHz when port 1 is driven

obtained using an Agilent N5230A vector network analyzer and anechoic chamber. As shown in Figure 7, there is a good agreement between the measured and simulated values of $|S_{11}|$ and $|S_{21}|$. A fractional bandwidth of 35.7% (from 690 MHz to 990 MHz) for $|S_{11}| < -15$ dB and an isolation of more than 28 dB were achieved. As shown in Figure 8, the antenna gain is stable around 8.65 dBi with a variation in 0.35 dBi. The 3 dB-beamwidth (HPBW) is $65.5 \pm 3.5^\circ$ in the H -plane (YOZ plane). The results for the H -plane are given for the geometric symmetry of the antenna. Figure 9 illustrates very stable radiation patterns at

700 MHz, 850 MHz, and 950 MHz for the H -plane and V -plane (XOZ plane). The measured results agree well with the simulated ones.

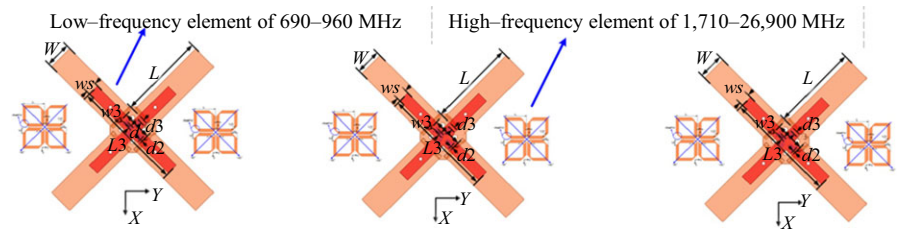
4 | FIVE-ELEMENT ANTENNA ARRAY

4.1 | Antenna design

In an actual base station, a high gain, stable HPBW in the H -plane ($65 \pm 5^\circ$), narrow radiation in the V -plane, and electrical

TABLE 2 Measured HPBW(*H*-Plane) and gain of the antenna array with different downtilts

Fre (MHz)	HPBW (deg)			Antenna gain (dBi)		
	0°	7°	14°	0°	7°	14°
698	70.0	69.8	69.4	13.3	13.4	13.2
750	68.6	69.6	69.2	13.7	13.5	13.3
790	67.5	68.5	68.8	14.0	14.0	13.8
820	67.0	67.8	68.5	13.6	13.5	13.5
870	65.3	65.8	65.7	14.1	14.0	14.1
920	65.2	65.4	66.1	14.3	14.4	14.2
960	60.2	66.4	66.7	13.6	13.8	13.4

**FIGURE 13** Schematic diagram of multiarray antenna**TABLE 3** Antenna gain with various higher band element spaces

Element space	$0.7 \times \lambda_{2.2\text{GHz}}$	$0.8 \times \lambda_{2.2\text{GHz}}$	$0.9 \times \lambda_{2.2\text{GHz}}$	$\lambda_{2.2\text{GHz}}$
Gain (dBi)	13.2	13.6	13.9	13.7

downtilt are needed. A five-element antenna array is presented for application in a modern base station. The antenna element space is 250 mm ($0.69\lambda_0$, where λ_0 is the free-space wavelength at 820 MHz). This space is two times the distance of the higher band element in the multiarray. Two-phase shifters are used in the five-element antenna array to realize an electrical downtilt of 0° to 14°. Compared with the traditional mechanical downtilt, the electrical downtilt has the advantage of obtaining more stable radiation patterns with different downtilts. Furthermore, it is easier to control the electrical downtilt. A prototype was fabricated to verify the proposed antenna design, as shown in Figure 10.

4.2 | Antenna performance

The simulated and measured S parameters of the antenna array are shown in Figure 11. The measured results indicate a wide impedance bandwidth of 34.7% (690 MHz to 980 MHz), and an isolation of more than 23 dB over the entire band. The measured HPBW (*H*-plane) and gain with different electrical downtilts are listed in Table 2. It is clear that a stable HPBW of $65 \pm 5^\circ$ is achieved with downtilts of 0°, 7°, and 14°. In addition, the antenna gains are 13.8 ± 0.5 dBi, 13.9 ± 0.5 dBi, and 13.7 ± 0.5 dBi for downtilts of 0°, 7°, and 14°, respectively. The simulated and measured radiation patterns with different electrical downtilts at 698 MHz, 820 MHz, and 960 MHz are shown in Figure 12. Very stable radiation patterns are obtained from 698 MHz to 960 MHz with electrical downtilts of 0°, 7°, and 14°. The measured results agree well with the simulated ones. All the results are shown when port 1 is driven because of the symmetric structure of the antenna array.

TABLE 4 Comparison with existing antennas

Antennas	Application for multiarray	Antenna size (mm × mm)	Fractional bandwidth	Gain (dBi)	Isolation (dB)	HPBW (deg)
In [6]	No	$1.17\lambda_0 \times 1.17\lambda_0 \times 0.21\lambda_0$	45.5% (VSWR < 2.0)	9.7	38	~70
In [7]	No	$1.06\lambda_0 \times 2.2\lambda_0 \times 0.254\lambda_0$	57.5% (VSWR < 1.5)	8.8 ± 0.3	31	81.2 ± 4.3
In [8]	No	$1.115\lambda_0 \times 1.115\lambda_0 \times 0.25\lambda_0$	52% (VSWR < 1.5)	7.8 ± 0.8	35	Not given
In [9]	Yes	Not given	21.2% (VSWR < 2.0)	~8.8	31	Not given
Our work	Yes	$0.94\lambda_0 \times 0.94\lambda_0 \times 0.245\lambda_0$	35.7% (VSWR < 1.5)	8.65 ± 0.35	28	65 ± 5

4.3 | Application of multiarray base station antenna

A schematic diagram of the multiarray based on the proposed dual-polarized antenna is presented in Figure 13. It is observed that sufficient space can be reserved for the higher frequency element using the cross-type dual-polarized antenna in the multiarray antenna. For an antenna array, the higher band element is more sensitive for mutual coupling because the wavelength is much more shorter. Table 3 shows the maximum gain with various higher element spaces for a three-element higher frequency antenna array. It is clear that the antenna achieved 13.9 dBi when the space was $0.9 \times \lambda_{2.2\text{GHz}}$ (123 mm). Therefore, the space of the higher band element is about $0.9 \times \lambda_{2.2\text{GHz}}$ and that of the lower band element space is about $0.69 \times \lambda_{0.82\text{GHz}}$. Thus, the multiarray antenna based on our proposed lower band antenna achieved improved antenna properties, to some extent, at the expense of lower band antenna gain.

5 | CONCLUSION

A wideband dual-polarized antenna with cross resonator has been proposed based on our novel concept of multimode filters. By adding the cross resonator, a new resonant mode was induced and the impedance matching was greatly improved. The resonance and input impedance can be adjusted by changing the size and position of the resonator. As a result, multiresonance and improved impedance matching were achieved over the desired operating band. A fractional bandwidth of 35.7% (from 690 MHz to 990 MHz) for $|S_{11}| < -15$ dB was achieved. In addition, stable gain and radiation patterns were obtained. A five-element antenna array was developed with an electrical downtilt of 0° to 14° for base station application. A stable HPBW of $65 \pm 5^\circ$ and a high gain of 13.8 ± 0.6 dBi were achieved with electrical downtilts of 0° , 7° , and 14° over the band of 690 MHz to 980 MHz ($|S_{11}| < -15$ dB). Comparisons with related previous works are given in Table 4. All the results show that the proposed antenna is a promising choice for LTE700/GSM800/GSM900 and 2G/3G/4G/5G multiarray base station applications.

ACKNOWLEDGMENTS

The authors appreciate the editor and reviewers' valuable comments and suggestions to our manuscript. This work was supported by the China Postdoctoral Science Foundation (2018M643084).

ORCID

Rui Wu  <https://orcid.org/0000-0001-9758-4281>

Qing-Xin Chu  <https://orcid.org/0000-0002-5807-0365>

REFERENCES

1. W. L. Stutzman, G. A. Thiele, *Antenna theory and design*, 3rd ed., Wiley, Hoboken, NJ, 2012.
2. C. A. Balanis, *Antenna theory analysis and design*, Wiley, Hoboken, NJ, 2005.
3. K. L. Wong, *Compact and broadband microstrip antennas*, Wiley, Hoboken, NJ, 2002.
4. Z.-N. Chen, K.-M. Luk, *Antennas for base stations in wireless communications*, McGraw-Hill, New York, NY, 2009.
5. R. Wu, Q. X. Chu, A broadband dual-polarized antenna with chamfers, *Microw. Opt. Technol. Lett.* **59** (2017), no. 3, 631–635.
6. B. Li et al., Wideband dual-polarized patch antenna with low cross polarization and high isolation, *IEEE Trans. Antennas Propag. Lett.* **11** (2012), 427–430.
7. Z. Bao, Z. Nie, X. Zong, A novel broadband dual-polarization antenna utilizing strong mutual coupling, *IEEE Trans. Antennas Propag.* **62** (2014), no. 1, 450–454.
8. Y. Gou et al., A compact dual-polarized printed dipole antenna with high isolation for wideband base station applications, *IEEE Trans. Antennas Propag.* **62** (2014), no. 8, 4392–4395.
9. S. Chen, K. M. Luk, High performance dual-band dual-polarized magneto-electric dipole base station antenna, *Asia-Pacific Microw. Conf.*, Sendai, Japan, Nov. 4–7, 2014, pp. 321–323.
10. H. Huang, Y. Liu, S. Gong, A broadband dual-polarized base station antenna with anti-interference capability, *IEEE Antennas Wireless Propag. Lett.* **16** (2017), 613–616.
11. Y.-H. Cui, R. Li, H. Fu, A broadband dual-polarized planar antenna for 2G/3G/LTE base stations, *IEEE Trans. Antennas Propag.* **62** (2014), no. 9, 4836–4840.
12. Z. Liu et al., A novel dual-Band and high-Gain antenna for 2G/3G base station, *Progress Electromagnetics Research Lett.* **54** (2015), 1–6.
13. Y. Cui, R. Li, P. Wang, Novel dual-broadband planar antenna and its array for 2G/3G/LTE base stations, *IEEE Trans. Antennas Propag.* **61** (2013), no. 3, 1132–1139.
14. Y. He et al., A novel dual-band, dual-polarized, miniaturized and low-profile base station antenna, *IEEE Trans. Antennas Propag.* **63** (2015), no. 12, 5399–5408.
15. D. Samb et al., Development of ultra-broadband base station antenna for all mainstream LTE 700/800/900 MHz frequency bands, *Int. J. Antennas Propag.* **2014** (2014), 201914:1–201914:10.
16. Y. He, W. Tian, L. Zhang, A novel dual-broadband dual-polarized electrical downtilt base station antenna for 2G/3G applications, *IEEE Access.* **5** (2017), 15241–15249.
17. H. Huang, Y. Liu, S. Gong, A novel dual-broadband and dual-polarized antenna for 2G/3G/LTE base stations, *IEEE Trans. Antennas Propag.* **64** (2016), no. 9, 4113–4118.
18. R. Wu, Q. X. Chu, Resonator-loaded broadband antenna for LTE700/GSM850/GSM900 base stations, *IEEE Antennas Wireless Propag. Lett.* **16** (2017), 501–504.
19. R. Wu, Q. X. Chu, A wideband dual-polarized antenna for LTE700/GSM850/GSM900 applications, *IEEE Antennas Wireless Propag. Lett.* **16** (2017), 2098–2101.
20. H. W. Lai, K.-M. Luk, Design and study of wide-band patch antenna fed by meandering probe, *IEEE Trans. Antennas Propag.* **54** (2006), no. 2, 564–571.
21. R. Wu, Q. X. Chu, Multi-mode broadband antenna for 2G/3G/LTE/5G wireless communication, *Electron. Lett.* **54** (2018), no. 10, 614–616.

22. Q. X. Chu, Y. Luo, *A broadband unidirectional multi-dipole antenna with very stable beamwidth*, IEEE Trans. Antennas Propag. **61** (2013), no. 5, 2847–2852.
23. D. L. Wen, D. Z. Zheng, Q. X. Chu, *A dual-polarized planar antenna using four folded dipoles and its array for base stations*, IEEE Trans. Antennas Propag. **64** (2016), no. 12, 5536–5542.
24. H. Huang, Y. Liu, S. Gong, *A novel dual-broadband and dual-polarized antenna for 2G/3G/LTE base stations*, IEEE Trans. Antennas Propag. **64** (2016), no. 9, 4113–4118.
25. K. M. Luk, H. Wong, *A new wideband unidirectional antenna element*, Microw. Opt. Technol. Lett. **1** (2006), no. 1, 2098–2101.
26. B. Q. Wu, K. M. Luk, *A broadband dual-polarized magneto-electric dipole antenna with simple feeds*, IEEE Antennas Wireless Propag. Lett. **8** (2009), 60–63.
27. AnsoftCorp, *HFSS*, available at <http://www.ansoft.com/products/hf/hfss>.

AUTHOR BIOGRAPHIES



Rui Wu was born in Hubei, China. He received his PhD degree from the Engineering Center of Antennas and RF Techniques of Guangdong Province at South China University of Technology, Guangzhou,

Guangdong, China. Currently, he works as a post-doctoral research fellow with the “Millimeter Wave and Terahertz Technical team” at South China University of Technology. His research interests include antennas in new generation mobile communications, wideband antennas, multiarray antennas, circularly polarized, and base station antennas.



Qing-Xin Chu received his BS, ME, and PhD in electronic engineering from Xidian University, Xi'an, Shaanxi, China, in 1982, 1987, and 1994, respectively. Currently, he is a professor with the School of

Electronic and Information Engineering, the director of the Research Institute of Antennas and RF Techniques, and the director of the Engineering Center of Antennas and RF Techniques of Guangdong Province at the South China University of Technology. He is also associated with the Xidian University as a distinguished professor in the Shaanxi Hundred-Talent Program since 2011. He was with the School of Electronic Engineering, Xidian University from Jan. 1982 to Jan. 2004, and he was a professor and the vice dean of the School of Electronic Engineering, Xidian University from Dec. 1997 to Jan. 2004. He is the foundation chair of IEEE Guangzhou AP/MTT Chapter, the vice-chair of China Electronic Institute (CEI) Antenna Society, an IEEE senior member, and a CEI (China Electronic Institute) fellow. He has published over 400 papers in journals and conferences with over 3000 SCI citations. Three of his papers that were published in IEEE Transactions on Antennas and Propagation or Microwave Theory and Techniques since 2008 became the top ESI (Essential Science Indicators) papers, and he was elected as a highly cited scholar by Elsevier in the field of Electrical and Electronic Engineering in 2014, 2015, and 2016. He has authored more than 40 invention patents of China. He was the recipient of the Science Award by CEI in 2016, the Science Award by Guangdong Province of China in 2013, the Science Awards by the Education Ministry of China in 2008 and 2002, the Fellowship Award by Japan Society for Promotion of Science (JSPS) in 2004, the Singapore Tan Chin Tuan Exchange Fellowship Award in 2003, and the Educational Award by Shaanxi Province in 2003. His current research interests include antennas and microwave filters in wireless communication, spatial power combining technology, and numerical techniques in electromagnetics.